

Macroscopic singlet states for gradient magnetometryIñigo Urizar-Lanz,¹ Philipp Hyllus,¹ Iñigo Luis Egusquiza,¹ Morgan W. Mitchell,^{2,3} and Géza Tóth^{1,4,5,*}¹*Department of Theoretical Physics, University of the Basque Country UPV/EHU, P.O. Box 644, E-48080 Bilbao, Spain*²*ICFO-Institut de Ciències Fòniques, Mediterranean Technology Park, E-08860 Castelldefels (Barcelona), Spain*³*ICREA-Institució Catalana de Recerca i Estudis Avançats, E-08015 Barcelona, Spain*⁴*IKERBASQUE, Basque Foundation for Science, E-48011 Bilbao, Spain*⁵*Wigner Research Centre for Physics, Hungarian Academy of Sciences, P.O. Box 49, H-1525 Budapest, Hungary*

(Received 19 April 2013; published 17 July 2013)

We present a method for measuring magnetic field gradients with macroscopic singlet states realized with ensembles of spin- j particles. While the singlet state is completely insensitive to homogeneous magnetic fields, the variance of its collective spin components is highly sensitive to field gradients. We compute the dynamics of this variance analytically for a chain of spins and also for an ensemble of particles with a given density distribution. We find an upper bound on how precisely the field gradient can be estimated from the measured data. Based on our calculations, differential magnetometry can be carried out with cold atomic ensembles using a multipartite singlet state obtained via spin squeezing. On the other hand, comparing the metrological properties of the experimentally prepared state to that of the ideal singlet can be used as further evidence that a singlet state has indeed been created.

DOI: [10.1103/PhysRevA.88.013626](https://doi.org/10.1103/PhysRevA.88.013626)

PACS number(s): 03.75.-b, 42.50.Dv, 42.50.Lc, 07.55.Ge

I. INTRODUCTION

Realization of large coherent quantum systems is at the center of attention in quantum experiments with cold atoms [1,2] and trapped ions [3]. Besides creating large-scale entanglement, it is also important to look for quantum information processing applications of the states created. Recently, a series of experiments has been carried out with cold atomic ensembles using spin squeezing [4]. This approach makes it possible to entangle 10^6 – 10^{12} atoms with each other by making them interact with a light field and then measuring the light, realizing in this way a quantum nondemolition (QND) measurement of one of the collective spin components [5,6]. Spin squeezed states are useful for continuous variable quantum teleportation [7] and magnetometry [8–13]. In these experiments, the atomic ensembles were almost completely polarized, which makes it possible to map the quantum state of these ensembles to the state of bosonic modes [14] and model, with few variables even, realistic dynamics including noise [15–18].

A basic scheme for magnetometry with an almost completely polarized spin squeezed state works as follows. The total spin of the ensemble is rotated by a magnetic field perpendicular to it. The larger the field, the larger the rotation, which allows one to obtain the field strength by measuring a spin component perpendicular to the mean spin. So far, it looks as if the mean spin behaves like a clock arm and its position will tell us the value of the magnetic field exactly. However, at this point, one has to remember that we have an ensemble of particles governed by quantum mechanics, and the uncertainty of the spin component perpendicular to the mean spin is never zero. Spin squeezing [19–22] can decrease the uncertainty of one of the perpendicular components and this can be used to increase the precision of the magnetometry [6].

Often the interesting quantity is not the absolute strength of the magnetic field but its gradient, and the effect of the homogenous field must be suppressed. For example, the magnetic field of Earth must be suppressed when the much smaller magnetic field around an electric device or magnetic structure is measured [23]. The field gradient can be determined by differential magnetometry, which can be carried out when two completely polarized atomic ensembles are used. In fact, the same light beam can pass through the two atomic ensembles, which can be used both for simultaneous spin squeezing of the two atomic ensembles and to carry out the differential measurement [8,9]. In general, singlet states of two large spins also offer the possibility for differential magnetometry [24].

It has recently been shown that interesting quantum states can be obtained even in unpolarized ensembles. In particular, if the uncertainties of the three collective angular momentum components are squeezed one after the other, then a multiparticle singlet state can be obtained [25,26]. (For other approaches creating singlet states of cold atoms, see Refs. [27–29].) Singlets, as ground states of antiferromagnetic Heisenberg spin systems, have attracted considerable attention [30–34]. Such states are invariant under the action of homogenous magnetic fields. On the other hand, a magnetic field gradient rotates the spins at different locations differently, which leads to the gradual destruction of the singlet state. During this process, the variance of the collective spin components is increasing and this fact can be used to measure the field gradient. The advantage of this method is that only a single ensemble is used for differential magnetometry, rather than two ensembles, which leads to a better resolution and also eases the experimental requirements of the method. The basic scheme for differential magnetometry with singlets is depicted in Fig. 1. (Other methods for measuring the field gradient can be found, for example, in Refs. [35–39].)

Besides demonstrating the usefulness of multiparticle singlets for metrology, our findings are interesting also to make singlets “visible” in an experiment. An insensitivity to

*toth@alumni.nd.edu; URL: <http://www.gtoth.eu>

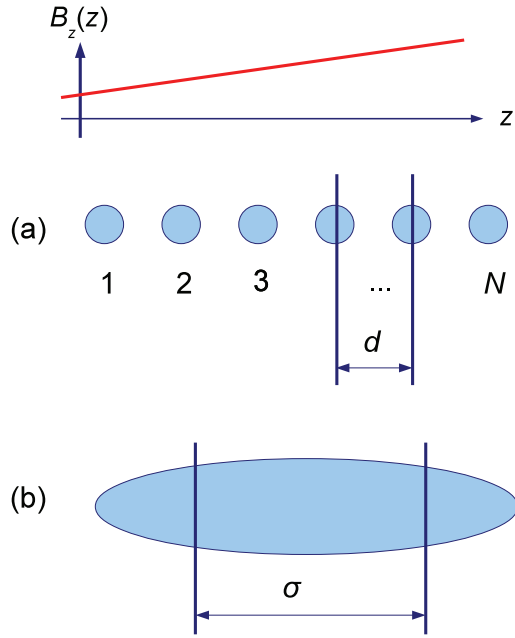


FIG. 1. (Color online) Multiqubit singlet in a field gradient. (a) Equidistant chain of N particles. (b) Atomic ensemble with a Gaussian density profile.

homogenous fields and a growing angular momentum variance due to a field gradient can be strong evidence that a singlet state has indeed been created. If we change the sign of the gradient, then the variances should start to decrease. Such a gradient echo experiment can be another way to analyze singlets. The accuracy of the magnetic field gradient measurement achieved in an experiment can also be compared to our calculations, and such a comparison could be used as further evidence that a singlet has been created.

Finally, our calculations are interesting from the theoretical point of view since we succeed in modeling the quantum dynamics of large atomic ensembles analytically. This is a surprise as quantum systems with millions of particles are typically difficult to model.

While we mainly discuss spin- $\frac{1}{2}$ particles, the spin squeezing procedure creating singlets and the differential metrology presented in our paper work also for spin- j particles for $j > \frac{1}{2}$. This is very important as looking for applications of ensembles of spin- j particles without restricting the dynamics to the spin- $\frac{1}{2}$ subspace is at the center of attention recently from the point of view of experiments and experimental proposals [11,25,40–47], and also from the point of view of spin squeezing entanglement criteria [48–54].

Our paper is organized as follows. In Sec. II, we describe the multiparticle singlet state of spin- $\frac{1}{2}$ particles and analyze its properties. In Sec. III, we calculate the dynamics of the variance of collective angular momentum components for such states under a magnetic field gradient for a singlet realized with a spin chain, shown in Fig. 1(a). We also compute bounds on the precision of the gradient measurements. In Sec. IV, we present calculations for an atomic ensemble with a given density profile, depicted in Fig. 1(b). In Sec. V, we consider the case of the singlet state mixed with noise and present results

for particles with a spin larger than $\frac{1}{2}$. Finally, we conclude the article in Sec. VI.

II. Multiparticle singlet states

In this section, we present an efficient description of multiparticle singlet states of N spin- $\frac{1}{2}$ particles.

Pure multiparticle singlet states are eigenstates of J_l with a 0 eigenvalue for $l = x, y, z$. Here, the collective operators are defined as

$$J_l = \sum_{n=1}^N j_l^{(n)}, \quad (1)$$

where $j_l = \frac{\hbar}{2}\sigma_l$ with the Pauli spin matrices σ_l for $l = x, y, z$. Due to this, pure multiparticle singlet states are invariant under the unitary transformations

$$U_{\vec{n}}(\theta) = \exp\left(-i\frac{J_{\vec{n}}}{\hbar}\theta\right), \quad (2)$$

where the angular momentum component along the \vec{n} direction is

$$J_{\vec{n}} = n_x J_x + n_y J_y + n_z J_z. \quad (3)$$

Such unitary transformations can be written as $U_{\vec{n}}(\theta) = u^{\otimes N}$, where $u = \exp(-i\frac{\theta}{\hbar}\sum_l n_l j_l)$.

Mixed multiparticle singlet states are mixtures of pure multiparticle singlets. Hence, multiparticle singlets give zero for the expectation values of all moments of all collective angular momentum components,

$$\langle J_l^m \rangle = 0, \quad (4)$$

where $l = x, y, z$ and $m = 1, 2, \dots, N$. Mixed multiparticle singlets are also invariant under the transformations of the type given by Eq. (2).

In summary, singlet states are the states within the zero subspace of the Hamiltonian

$$H_s = \kappa(J_x^2 + J_y^2 + J_z^2), \quad (5)$$

where $\kappa > 0$ is a constant. The dimension of this space is growing rapidly with N [55]. We have to identify the singlet created in the spin squeezing procedure in this space.

A. Determining the singlet obtained in spin squeezing experiments

In this section, we determine the multiparticle singlet created by spin squeezing procedures. Due to symmetries of the setup, the state created is permutationally invariant. There are very many multiparticle singlets. We will now show that, on the other hand, there is a unique permutationally invariant singlet.

Permutational invariance means that the quantum state ρ equals its permutationally invariant part,

$$(\rho)_{\text{PI}} = \frac{1}{N!} \sum_{k=1}^{N!} \Pi_k \rho \Pi_k^\dagger, \quad (6)$$

where Π_k is a permutation operator and the summation is over all permutations. The singlet state realized by the squeezing procedure in an atomic ensemble is permutationally invariant

for the following reasons. First, it is created starting from the completely mixed state, which is permutationally invariant. Second, the measurement-feedback procedure to squeeze the collective variables involves only collective, not individual, variables. Hence, the dynamics is completely symmetric under exchange of particles [25].

Hence, we can state the following.

Observation 1. For a given even number of particles N , there is a unique permutationally invariant singlet state. It can be expressed as

$$\rho_s = \lim_{T \rightarrow 0} \frac{e^{-\frac{H_s}{T}}}{\text{Tr}(e^{-\frac{H_s}{T}})} \quad (7)$$

and

$$\rho_s = (|\Psi^-\rangle\langle\Psi^-| \otimes \cdots \otimes |\Psi^-\rangle\langle\Psi^-|)_{\text{PI}}, \quad (8)$$

where the operation $(X)_{\text{PI}}$ is defined in Eq. (6) and the two-particle singlet is

$$|\Psi^-\rangle = \frac{1}{\sqrt{2}} \left(\left| +\frac{1}{2}, -\frac{1}{2} \right\rangle_z - \left| -\frac{1}{2}, +\frac{1}{2} \right\rangle_z \right), \quad (9)$$

where $|\pm\frac{1}{2}\rangle_z$ are the eigenstates of J_z .

Proof. First we will show that there is a unique permutationally invariant singlet state. Such states have the following properties: (i) they are permutationally invariant and (ii) they are the eigenstates of J_l for $l = x, y, z$ with eigenvalues 0. All permutationally invariant multiparticle states are uniquely characterized by the expectation values $\langle A^{\otimes(N-n)} \otimes \mathbb{1}^{\otimes n} \rangle$, where $n = 0, 1, 2, \dots, N-1$ and A is a traceless single-particle operator [56]. Moreover, as discussed before, all states for which $J_l = 0$ for $l = x, y, z$ are invariant under the transformations of the type $u^{\otimes N}$, where u are unitary matrices acting on a single spin. Since any traceless A can be obtained from σ_z by unitaries, such a state can be uniquely characterized by the N expectation values $\langle \sigma_z^{\otimes(N-n)} \otimes \mathbb{1}^{\otimes n} \rangle$, where $n = 0, 1, 2, \dots, N-1$. Knowing these expectation values is the same as knowing the expectation values of the powers J_z^n , for $n = 1, 2, \dots, N$. However, these expectation values are zero for all singlets, as can be seen in Eq. (4). Thus, there is a single permutationally invariant singlet state, and Eqs. (7) and (8) are indeed equal [57]. ■

Let us interpret first the Eq. (7) formula. It denotes a state that is a completely mixed state within the $\sum_l \langle J_l^2 \rangle = 0$ subspace. It can also be written as

$$\rho_s = \frac{1}{d_0} \sum_{\alpha=1}^{d_0} |0, 0, \alpha\rangle\langle 0, 0, \alpha|, \quad (10)$$

where $|j, j_z, \alpha\rangle$ denotes a state for which $\sum_l J_l^2 |j, j_z, \alpha\rangle = j(j+1)|j, j_z, \alpha\rangle$, $J_z |j, j_z, \alpha\rangle = j_z |j, j_z, \alpha\rangle$, α is used to label the degenerate eigenstates, and d_0 is the degeneracy of the $j = j_z = 0$ eigenstate [55].

An alternative expression for the permutationally invariant singlet is given in Eq. (8). It shows that the multiparticle singlet is an equal mixture of all tensor products of two-particle singlets [58]. One can even find that for an even N , the number of different permutations of such a singlet chain is [59]

$$f(N) = (N-1)!! = (N-1)(N-3)(N-5)\cdots \quad (11)$$

This fact has very important consequences for modeling quantum systems in such a state. While storing the density matrix for a general quantum state of many particles is impossible, storing a representation of a product state or a state that is a product of few-particle units can be done efficiently. In the next sections, we will explain how to compute quantum dynamics starting from the permutationally invariant multiparticle singlet state.

B. Calculating the reduced states of the singlet

In this section, we will calculate ρ_1^{red} , ρ_{12}^{red} , and ρ_{1234}^{red} , which are, respectively, the reduced one-particle, two-particle, and four-particle density matrices of the singlet state ρ_s . Later, this will be needed when computing the time evolution of certain operators for the singlet state.

We have to start from the decomposition given by Eq. (8). From that, we obtain the form

$$\rho_{1234}^{\text{red}} = \left(\alpha \frac{\mathbb{1}}{16} + \beta |\Psi_{12}^-\rangle\langle\Psi_{12}^-| \otimes |\Psi_{34}^-\rangle\langle\Psi_{34}^-| + \gamma |\Psi_{12}^-\rangle\langle\Psi_{12}^-| \otimes \frac{\mathbb{1}}{4} + \text{permutations} \right), \quad (12)$$

where the second term has altogether three different permutations, while the third term has six different permutations [including those appearing in Eq. (12)]. The term multiplied by β is obtained when the particles 1 to 4 are in a product of two singlet states. The number of times that this special order is reached is given by the number of ways to distribute the remaining $(N-4)$ particles in $(N-4)/2$ pairs, that is, $(N-4-1)!!$. This has to be divided by the number of all distributions, that is, $(N-1)!!$. Hence, we obtain

$$\beta = \frac{(N-4-1)!!}{(N-1)!!} = \frac{1}{(N-1)(N-3)}. \quad (13)$$

The term multiplied by γ is obtained when the particles 1 and 2 are in a singlet state, but particles 3 and 4 are not. As above, the number of times the remaining $N-2$ particles can be distributed in pairs is $(N-2-1)!!$. However, we have to subtract here the number of distributions where particles 3 and 4 are in a singlet state as well, that is, $(N-4-1)!!$, as shown above. Again, we have to divide this by the total number of distributions, $(N-1)!!$, arriving at

$$\begin{aligned} \gamma &= \frac{(N-2-1)!!}{(N-1)!!} - \frac{(N-4-1)!!}{(N-1)!!} \\ &= \frac{1}{(N-1)} - \frac{1}{(N-1)(N-3)}. \end{aligned} \quad (14)$$

Finally, for the coefficient of the completely mixed component, we have

$$\alpha = 1 - 3\beta - 6\gamma. \quad (15)$$

This occurs when all four particles are in a singlet state with particles outside this set.

The two-spin reduced density matrix can be obtained from Eq. (12) by tracing out particles 3 and 4 as

$$\rho_{12}^{\text{red}} = \text{Tr}_{34}(\rho_{1234}^{\text{red}}) = p_s |\Psi_{12}^-\rangle\langle\Psi_{12}^-| + (1-p_s) \frac{\mathbb{1}}{4}, \quad (16)$$

where

$$p_s = \beta + \gamma = \frac{1}{N-1}, \quad (17)$$

which can also be obtained from combinatorial calculations similar to the ones carried out for β as $(N-3)!!/(N-1)!!$. Finally, this leads to the trivial single-spin reduced state

$$\rho_1^{\text{red}} = \frac{\mathbb{1}}{2}. \quad (18)$$

III. Gradient magnetometry with a multiparticle spin chain

In this section, we consider N spin- $\frac{1}{2}$ particles in a permutationally invariant singlet state of Eq. (8), where the particles are confined to a one-dimensional array. This could be prepared, for instance, with a Bose-Einstein condensate in an optical lattice driven to the so-called Mott-insulator state [60,61].

We will calculate the effect of the magnetic field gradient on the singlet. In particular, we will calculate how the variance of the collective angular momentum components increases with the application of the field gradient. We will also calculate how precisely the field gradient can be estimated from the measured data.

In our calculations, we consider a one-dimensional array along the z direction, such that the positions of the particles are given by

$$(x_n, y_n, z_n) = (0, 0, z_n^c), \quad (19)$$

where $n = 1, 2, \dots, N$. A particular example is the equidistant chain where

$$z_n^{\text{ce}} = (n-1)d + z_0, \quad (20)$$

d is the distance between the particles, and z_0 is an offset. This situation is depicted in Fig. 1. We collect the positions on the z axis in the vector \vec{z}_N^c .

We can write the field at the atoms, situated along $x = y = 0$, as

$$\mathbf{B}(0,0,z) = \mathbf{B}_0 + z\mathbf{B}_1 + O(z^2), \quad (21)$$

where we will neglect the terms of order two or higher. We will consider $\mathbf{B}_0 = B_0(0,0,1)$ and $\mathbf{B}_1 = B_1(0,0,1)$. For this configuration, due to the Maxwell equations, for the case of no currents or changing electric fields, we have

$$\text{div } \mathbf{B} = 0, \quad \text{curl } \mathbf{B} = \mathbf{0}.$$

This implies $\sum_{l=x,y,z} \partial B_l / \partial l = 0$ and $\partial B_l / \partial m - \partial B_m / \partial l = 0$ for $l \neq m$. Thus, the spatial derivatives of the field components are not independent of each other. However, in the case of a linear chain only, the derivative along the chain has an influence on the quantum dynamics of the atoms. A similar statement holds for a quasi-one-dimensional atomic ensemble, which is typically the case if we consider an elongated trap.

The Hamiltonian corresponding to the effect of a homogeneous magnetic field in the z direction is

$$H_{\hat{z}} = \gamma B_0 \sum_{n=1}^N j_z^{(n)}, \quad (23)$$

where γ is the gyromagnetic ratio. It gives rise to a time evolution given in Eq. (2) with $\vec{n} = \hat{z}$, where \hat{z} is the unit vector pointing in the z direction. As we have discussed before, multiparticle singlets are invariant under the transformations

of the type given by Eq. (2). On the other hand, the singlet is not invariant under the quantum dynamics generated by a magnetic field *gradient* B_1 described by the Hamiltonian

$$H_G = \gamma B_1 \sum_{n=1}^N z_n^c j_z^{(n)}, \quad (24)$$

where z_n^c is the position on the z axis of the spin n and B_1 is the field gradient along the z direction. Introducing a characteristic length L , the Hamiltonian (24) can be rewritten as

$$H_G = \omega_L \sum_{n=1}^N \left(\frac{z_n^c}{L} \right) j_z^{(n)}, \quad (25)$$

where $\omega_L = \gamma B_1 L$.

For instance, one may choose $L = d$ in the case of the equidistant chain described by Eq. (20). Introducing the normalized Hamiltonian $H'_G = \frac{H_G}{\omega_L}$ and

$$\Theta = \omega_L t, \quad (26)$$

the time evolution operator becomes

$$U_G(\Theta) = \exp \left[-i \frac{H'_G}{\hbar} \Theta \right]. \quad (27)$$

This formalism expresses the fact that our setup measures the field gradient times the time.

In order to use the singlet for differential magnetometry, we need to find an observable that changes with Θ . We investigate powers of collective operators J_l^m since these are relatively easy to measure experimentally. It is clear that $l = z$ is not a good choice because $[J_z, H'_G] = 0$, so this observable does not change with Θ . Therefore, we start by investigating whether the first or second moment of J_x might be a suitable candidate.

A. Calculating $\langle J_x \rangle$ and $\langle J_x^2 \rangle$

We compute the dynamics of $\langle J_x \rangle$ and $\langle J_x^2 \rangle$ starting from a multipartite singlet taking advantage of the fact that it is the mixture of all the permutations of tensor products of two-particle singlets, as can be seen in Eq. (8). We will work in the Heisenberg picture; thus all operators will be given as a function of Θ , while expectation values will be computed for the initial state ϱ_s . Hence the time evolution of the operator J_x is given with the time-dependent single-spin operators as

$$J_x(\Theta) = \sum_n j_x^{(n)}(\Theta). \quad (28)$$

1. Chain of particles at arbitrary positions

In this part, we will carry out calculations for a chain of particles at arbitrary positions. In the next part, we will present results for the equidistant chain.

In the Heisenberg picture, the time dependence of an operator A is given as

$$A(\Theta) = \exp \left(i \frac{H'_G}{\hbar} \Theta \right) A \exp \left(-i \frac{H'_G}{\hbar} \Theta \right). \quad (29)$$

Hence, for the time dependence of the single-particle operator $j_z^{(n)}$, we obtain

$$j_x^{(n)}(\Theta) = c_n j_x^{(n)} - s_n j_y^{(n)} \equiv X_{\Theta}^{(n)}, \quad (30)$$

where we introduced the notation

$$c_n = \cos\left(\frac{z_n^c}{L}\Theta\right) \text{ and } s_n = \sin\left(\frac{z_n^c}{L}\Theta\right). \quad (31)$$

The quantities c_n and s_n are the cosine and sine of the phases picked up by the n th particle. The expectation value of J_x is therefore given by

$$\langle J_x \rangle_s^{\bar{z}_N^c}(\Theta) = \sum_n (c_n \langle j_x^{(n)} \rangle_{\rho_1^{\text{red}}} - s_n \langle j_y^{(n)} \rangle_{\rho_1^{\text{red}}}) = 0 \quad (32)$$

because the single-particle reduced state of the singlet ρ_s is the completely mixed state; cf. Eq. (18). Note that the reduced state ρ_1^{red} is the same for any n since ρ_s is permutationally invariant.

In analogy, it can be shown that $\langle J_y \rangle_s^{\bar{z}_N^c}(\Theta) = 0$. Therefore, a measurement of J_l is not suitable for estimating Θ for $l = x, y, z$. We continue by investigating whether a measurement of J_x^2 is useful.

We can write J_x^2 in the Heisenberg picture [cf. Eqs. (28) and (29)] as a sum over two variables. Knowing that $(X_\Theta^{(n)})^2 = \frac{1}{4}$, we can write the expectation value of the second moment of J_x as a sum of a constant and two-body correlations as

$$\langle J_x^2 \rangle_s^{\bar{z}_N^c}(\Theta) = \frac{N}{4}\hbar^2 + \sum_{n_1 \neq n_2} \langle X_\Theta^{(n_1)} X_\Theta^{(n_2)} \rangle_{\rho_s}. \quad (33)$$

In the following, we will partly drop the index \bar{z}_N^c and sometimes also Θ from $\langle J_x^2 \rangle_s^{\bar{z}_N^c}(\Theta)$ when there is no risk of confusion. Since the singlet state is permutationally invariant, the correlation term on the right-hand side of Eq. (33) can be rewritten with the two-particle reduced state of the singlet as

$$\begin{aligned} & \sum_{n_1 \neq n_2} \langle X_\Theta^{(n_1)} X_\Theta^{(n_2)} \rangle_{\rho_s} \\ &= \sum_{n \neq m} \langle (c_n j_x^{(1)} - s_n j_y^{(1)})(c_m j_x^{(2)} - s_m j_y^{(2)}) \rangle_{\rho_{12}^{\text{red}}}. \end{aligned} \quad (34)$$

In Sec. II B, we obtained ρ_{12}^{red} , the reduced two-spin state of the singlet [cf. Eq. (16)]. Direct calculation shows that

$$\langle j_k \otimes j_l \rangle_{\rho_{12}^{\text{red}}} = -\frac{\hbar^2}{4(N-1)}\delta_{kl}, \quad (35)$$

where $k, l = x, y, z$ and δ_{kl} is 1 if the two indices are equal, otherwise it is 0. Substituting Eq. (35) into Eq. (34), we obtain the sum of the two-body correlations as

$$\sum_{n_1 \neq n_2} \langle X_\Theta^{(n_1)} X_\Theta^{(n_2)} \rangle_{\rho_s} = -\frac{\hbar^2}{4(N-1)}I_2, \quad (36)$$

where

$$I_2 \equiv \sum_{n \neq m} (c_n c_m + s_n s_m), \quad (37)$$

and therefore

$$\langle J_x^2 \rangle_s^{\bar{z}_N^c}(\Theta) = \frac{N\hbar^2}{4} \left[1 - \frac{1}{N(N-1)}I_2 \right]. \quad (38)$$

Since this is a nontrivial function of Θ , a measurement of J_x^2 can be used to estimate the magnetic field gradient.

Note that Eq. (38) contains a sum over two variables such that the two variables are not allowed to be equal. For practical

purposes, it is more useful to rewrite this with independent sums that require less computational effort as

$$I_2 = \sum_{n,m} (c_n c_m + s_n s_m) - \sum_n (c_n^2 + s_n^2) \equiv (C^2 + S^2 - N), \quad (39)$$

where we define the sums

$$C = \sum_n \cos\left(\frac{z_n^c}{L}\Theta\right), \quad S = \sum_n \sin\left(\frac{z_n^c}{L}\Theta\right), \quad (40)$$

and use that $c_n^2 + s_n^2 = 1$. A similar subtraction procedure can be used in a more complicated calculation for the fourth moment of an angular momentum component below [62]. Inserting Eq. (39) into Eq. (38), we can state the following.

Observation 2. The time dependence of the expectation value of the second moment of J_x , starting from a singlet of a chain of N particles with the z coordinates \bar{z}_N^c , is given by

$$\langle J_x^2 \rangle_s^{\bar{z}_N^c}(\Theta) = \frac{N\hbar^2}{4} \left\{ 1 + \frac{1}{N(N-1)}[N - C^2 - S^2] \right\}, \quad (41)$$

where C and S are defined in Eq. (40).

Due to the symmetries of the setup, the dynamics of the variance of the y component of the angular momentum is the same as the dynamics of the variance of the x component,

$$\langle J_y^2 \rangle_s(\Theta) = \langle J_x^2 \rangle_s(\Theta), \quad (42)$$

while $\langle J_z^2 \rangle_s(\Theta) = 0$ as mentioned before.

From Sec. II, we know that the singlet at $t = 0$ is invariant under the influence of any homogenous magnetic fields. For $t > 0$, this is not true any more. However, the singlet evolving under the influence of H_G given in Eq. (25) still remains invariant under the transformation $U_z(\theta) = \exp(-i\frac{J_z}{\hbar}\theta)$ since $[H_G, J_z] = 0$. Because of that, $\langle J_z^2 \rangle_s(\Theta) = 0$ for all Θ .

2. Equidistant chain

For the particular example of the equidistant chain, it is convenient to rewrite $\langle J_x^2 \rangle_s$ using the identity

$$c_n c_m + s_n s_m = \cos\left(\frac{z_n^c - z_m^c}{L}\Theta\right), \quad (43)$$

which, from Eqs. (38) and (39) and with the z coordinates z_n^c given in Eq. (20), leads to

$$\begin{aligned} & \langle J_x^2 \rangle_s(\Theta) \\ &= \frac{N\hbar^2}{4} \left(1 - \frac{1}{N(N-1)} \left\{ \sum_{n,m} \cos[(n-m)\Theta] - N \right\} \right), \end{aligned} \quad (44)$$

with the choice $L = d$.

The variance of J_x starts from zero as follows from the properties of the singlet state. It can also be seen from Eq. (44) because each of the N^2 terms in the sum is equal to 1 at $\Theta = 0$. Then the variance grows up to around the level of the completely mixed state (white noise) $\frac{1}{2N}$,

$$\langle J_x^2 \rangle_{\text{wn}} = \frac{N}{4}\hbar^2. \quad (45)$$

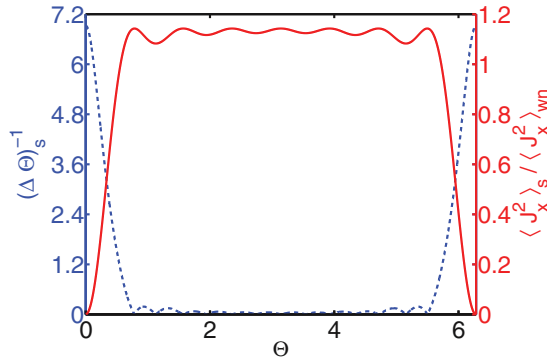


FIG. 2. (Color online) The dynamics of $\langle J_x^2 \rangle_s / \langle J_x^2 \rangle_{\text{wn}}$ (solid line) and $(\Delta\Theta)^{-1}$ (dashed line) as the function of Θ for an equidistant chain of $N = 8$ particles. The angular momentum variance for the white noise, $\langle J_x^2 \rangle_{\text{wn}}$, is defined in Eq. (45).

To be more precise, for even N ,

$$\langle J_x^2 \rangle_s(\Theta = \pi) = \frac{N\hbar^2}{4} \left[1 + \frac{1}{N-1} \right], \quad (46)$$

which is very close to $\langle J_x^2 \rangle_{\text{wn}}$ for large N . The reason for this is that $\sum_{n,m} \cos[(n-m)\pi] = 0$ because when N is even, the number of terms where $n-m$ is even (such that $\cos[(n-m)\pi] = +1$) is equal to the number of terms where $n-m$ is odd (such that $\cos[(n-m)\pi] = -1$). At $\Theta = 2\pi$, $\langle J_x^2 \rangle_s$ returns to 0 because again $\cos[(n-m)2\pi] = 1$ for all n and m since $n-m$ is an integer. Obviously, for the equidistant chain, $\langle J_x^2 \rangle_s(\Theta)$ is a periodic function with a period time

$$T = \frac{2\pi}{\omega_{L=d}} = \frac{2\pi}{\gamma B_1 d}. \quad (47)$$

If there is not a complete revival, then the particles are not arranged in an array such that the interparticle distance is uniform over the chain. This phenomenon can be used to characterize chains of atoms from the point of view of the uniformity of the distribution of the atoms.

In Fig. 2, we plot the dynamics of $\langle J_x^2 \rangle_s(\Theta)$ for $N = 8$ spin- $\frac{1}{2}$ particles. Note that the increase of $\langle J_x^2 \rangle_s$ is not monotonic for $\Theta < \pi$, but, rather, is oscillating. This is due to the fact that the atoms are arranged in a lattice. In the case of a continuous density distribution, there is no such oscillation, as will be shown in Sec. IV.

B. Calculating the precision of estimating Θ

From the calculation of $\langle J_x^2 \rangle_s(\Theta)$, it is clear that a measurement of J_x^2 gives information about Θ ; hence, it can be used to estimate an unknown value of Θ . In this section, we will calculate the precision $\Delta\Theta$ of the estimation, for the singlet state realized with a chain of spins with the z coordinates \vec{z}_N^c undergoing a quantum dynamics due to a magnetic field gradient.

The finite precision in reconstructing Θ comes from the fact that J_x^2 can only be measured with some uncertainty. The precision of the reconstruction of Θ based on measuring J_x^2 can be obtained as

$$(\Delta\Theta)_s^2 = \frac{(\Delta J_x^2)_s^2}{|\partial_\Theta \langle J_x^2 \rangle_s|^2}, \quad (48)$$

where $(\Delta A)^2 = \langle A^2 \rangle - \langle A \rangle^2$ for an observable A . In order to calculate the expression (48), we need to know $\langle J_x^2 \rangle_s(\Theta)$, which we have just obtained, and $\langle J_x^4 \rangle_s(\Theta)$, which we are going to calculate now.

Let us consider again the one-dimensional chain of particles. For this, the Hamiltonian is given in Eq. (25). As in Sec. III A, we will work again in the Heisenberg picture. The time evolution of the operator J_x^4 is

$$J_x^4(\Theta) = \left[\sum_n j_x^{(n)}(\Theta) \right]^4. \quad (49)$$

The expectation value of this can be rewritten as a sum over four variables as

$$\langle J_x^4 \rangle_s = \sum_{n_1, n_2, n_3, n_4} \langle X_\Theta^{(n_1)} X_\Theta^{(n_2)} X_\Theta^{(n_3)} X_\Theta^{(n_4)} \rangle_{\mathcal{E}_s}. \quad (50)$$

Again, we leave out the indices \vec{z}_N^c and Θ for simplicity at the moment. We can rewrite Eq. (50) with sums in which the variables of the summation are not allowed to be equal as

$$\begin{aligned} \langle J_x^4 \rangle_s &= \sum_{n_1} \langle (X_\Theta^{(n_1)})^4 \rangle_{\mathcal{E}_s} + 3 \sum_{n_1 \neq n_2} \langle (X_\Theta^{(n_1)})^2 (X_\Theta^{(n_2)})^2 \rangle_{\mathcal{E}_s} \\ &+ 4 \sum_{n_1 \neq n_2} \langle (X_\Theta^{(n_1)})^3 (X_\Theta^{(n_2)}) \rangle_{\mathcal{E}_s} \\ &+ 6 \sum_{\substack{n_1 \neq n_2, n_3 \\ \neq (n_1, n_2, n_3)}} \langle (X_\Theta^{(n_1)})^2 (X_\Theta^{(n_2)}) (X_\Theta^{(n_3)}) \rangle_{\mathcal{E}_s} \\ &+ \sum_{\substack{n_1 \neq n_2, n_3, n_4 \\ \neq (n_1, n_2, n_3, n_4)}} \langle X_\Theta^{(n_1)} X_\Theta^{(n_2)} X_\Theta^{(n_3)} X_\Theta^{(n_4)} \rangle_{\mathcal{E}_s}, \end{aligned} \quad (51)$$

where $\sum_{\neq(i,j,k)}$ denotes summation over the indices j, k, l such that none of them is equal to another one. Based on Eq. (51) and by making use of the fact that $\langle X_\Theta^{(n)} \rangle^2 = \frac{1}{4}\hbar^2$, we arrive at

$$\begin{aligned} \langle J_x^4 \rangle_s &= \frac{\hbar^4}{16} [N + 3N(N-1)] \\ &+ \hbar^2 \left[1 + \frac{3(N-2)}{2} \right] \sum_{n_1 \neq n_2} \langle X_\Theta^{(n_1)} X_\Theta^{(n_2)} \rangle_{\mathcal{E}_s} \\ &+ \sum_{\substack{n_1 \neq n_2, n_3, n_4 \\ \neq (n_1, n_2, n_3, n_4)}} \langle X_\Theta^{(n_1)} X_\Theta^{(n_2)} X_\Theta^{(n_3)} X_\Theta^{(n_4)} \rangle_{\mathcal{E}_s}. \end{aligned} \quad (52)$$

The expectation value of the sum of the two-body correlations is given in Eq. (36). Next, we calculate the expectation values for the four-body correlations. For that, we use the reduced four-particle density matrix presented in Eq. (12). For the reduced four-particle matrix, we obtain

$$\begin{aligned} \langle j_x^{(1)} j_x^{(2)} j_x^{(3)} j_x^{(4)} \rangle_{\mathcal{E}_{1234}^{\text{red}}} &= \frac{\hbar^4}{16} \frac{3}{(N-1)(N-3)}, \\ \langle j_y^{(1)} j_y^{(2)} j_y^{(3)} j_y^{(4)} \rangle_{\mathcal{E}_{1234}^{\text{red}}} &= \frac{\hbar^4}{16} \frac{3}{(N-1)(N-3)}, \end{aligned} \quad (53)$$

and

$$\langle j_x^{(1)} j_x^{(2)} j_y^{(3)} j_y^{(4)} \rangle_{\mathcal{E}_{1234}^{\text{red}}} = \frac{\hbar^4}{16} \frac{1}{(N-1)(N-3)}. \quad (54)$$

The singlet state is invariant under $U^{\otimes N}$ for any local unitary U . This leads to $\langle j_x^{(1)} j_y^{(2)} j_y^{(3)} j_y^{(4)} \rangle_{\mathcal{E}_{1234}^{\text{red}}} = \langle j_x^{(1)} j_x^{(2)} j_x^{(3)} j_x^{(4)} \rangle_{\mathcal{E}_{1234}^{\text{red}}} = 0$ [63]. Since the singlet is permutationally invariant, all the

expectation values with four-body correlations with j_x and j_y follow. Taking everything into account, we arrive at the expression

$$\langle J_x^4 \rangle_s = \frac{\hbar^4}{16} \left\{ 3N^2 - 2N - \frac{6N-8}{N-1} I_2 + \frac{3}{(N-1)(N-3)} I_4 \right\}, \quad (55)$$

where we defined

$$I_4 \equiv \sum_{\neq(k,l,m,n)} [c_k c_l c_n c_m + s_k s_l s_n s_m + 2c_k c_l s_n s_m]. \quad (56)$$

The term I_4 involves a sum over four variables, which implies a large computational effort for large systems. Similarly to what has been done with I_2 in Eq. (39), we can write I_4 as

$$I_4 = \sum_{k,l,n,m} [c_k c_l c_n c_m + s_k s_l s_n s_m + 2c_k c_l s_n s_m] - P. \quad (57)$$

In P , we will write all the terms that appear in $\sum_{k,l,n,m}$ but do not appear in $\sum_{\neq(k,l,m,n)}$. Let us study the first term of the right-hand side of Eq. (57). We can rewrite it as

$$\sum_{k,l,n,m} [c_k c_l c_n c_m + s_k s_l s_n s_m + 2c_k c_l s_n s_m] = C^4 + S^4 + 2C^2 S^2, \quad (58)$$

where C and S are defined in Eq. (40). Next, we have to determine P . After determining it, we have to eliminate the sums containing conditions that multiple indices are unequal in a similar manner by replacing the sum with another one without such a condition and subtracting the difference. Finally, we arrive at an expression with single-index sums only. Using these results, we obtain the following [62].

Observation 3. The time dependence of the expectation value of the fourth moment of J_x , starting from a singlet of a chain of N particles with the z coordinates \vec{z}_N^c , is given by

$$\langle J_x^4 \rangle_s^{\vec{z}_N^c}(\Theta) = \frac{\hbar^4}{16} \left\{ 3N^2 - 2N - \frac{6N-8}{N-1} I_2 + \frac{3}{(N-1)(N-3)} I_4 \right\}, \quad (59)$$

where I_2 and I_4 are defined in Eqs. (37) and (56) and can be rewritten as

$$\begin{aligned} I_2 &= X_{1,0}^2 + X_{0,1}^2 - N, \\ I_4 &= X_{1,0}^4 + X_{0,1}^4 + 2X_{1,0}^2 X_{0,1}^2 - 6X_{4,0} - 6X_{0,4} - 12X_{2,2} \\ &\quad + 3X_{2,0}^2 + 3X_{0,2}^2 + 8X_{3,0} X_{1,0} + 8X_{0,3} X_{0,1} + 4X_{1,1}^2 \\ &\quad + 8X_{2,1} X_{0,1} + 8X_{1,2} X_{1,0} + 2X_{2,0} X_{0,2} - 6X_{2,0} X_{1,0}^2 \\ &\quad - 6X_{0,2} X_{0,1}^2 - 2X_{2,0} X_{0,1}^2 - 2X_{0,2} X_{1,0}^2 - 8X_{1,1} X_{1,0} X_{0,1}, \end{aligned} \quad (60)$$

where

$$X_{k,l} = \sum_{n=1}^N c_n^k s_n^l, \quad (61)$$

with c_n and s_n as defined in Eq. (31).

Alternatively, it is possible to write the term I_4 in a more compact form as [62]

$$I_4 = N \left\{ 2(N-3) - 4N(N-2) |\hat{f}_1(\alpha)|^2 + N^3 |\hat{f}_1(\alpha)|^4 + N |\hat{f}_1(2\alpha)|^2 - 2N^2 \text{Re}[\hat{f}_1^2(\alpha) \hat{f}_1(2\alpha)^*] \right\}, \quad (62)$$

where

$$\hat{f}_1(\alpha) = \frac{1}{N} \sum_k e^{i\alpha z_k^c} \quad \text{and} \quad \alpha = \frac{\Theta}{L}, \quad (63)$$

which is also easier to compute.

Observations 2 and 3 make it possible to calculate the precision of the estimation $\Delta\Theta$ based on Eq. (48). It is possible to calculate analytically the precision for $\Theta = 0$. For that, we determined the zeroth- and first-order terms of the Taylor expansion of Eq. (48) using the expansion of sine and cosine up to second order. Hence, we can state the following.

Observation 4. The maximal precision of estimating $\Delta\Theta$ for an equidistant chain of N spin- $\frac{1}{2}$ particles is characterized by

$$(\Delta\Theta)_s^{-2}(\Theta = 0) = \frac{N^2 + N^3}{12} = \left[N \frac{\sigma^2}{L^2} \right] \frac{N}{N-1}, \quad (64)$$

where $\sigma = L\sqrt{(N^2-1)/12}$ is the standard deviation of the equidistant chain, and $L = d$.

A more general result on the precision at $\Theta = 0$ will be presented in Observation 7 below.

In Fig. 2, we plot the dynamics of $(\Delta\Theta)_s^{-1}$ for $N = 8$ for the equidistant chain. As can be seen, the precision is maximal at $\Theta = 0$. Then, it decreases; however, this decrease is not monotonic and the precision is oscillating. In particular, based on Eq. (48), one can see that the precision is zero when the tangent of $\langle J_x^2 \rangle_s(\Theta)$ is horizontal, i.e., $\partial_\Theta \langle J_x^2 \rangle_s(\Theta) = 0$.

IV. CONTINUOUS DENSITY PROFILE

In this section, we work out the formulas describing the case of a one-dimensional continuous density profile. We present the dynamics of the second and fourth moments of the collective angular momentum components for this case.

In the case of a spin chain, the particles were placed in the fixed positions \vec{z}_N^c . Now, while we still consider the case when the particles are localized in certain positions, the distribution of N particles is given by a distribution function f_N , where

$$f_N(z_1, z_2, \dots, z_N) dz_1 dz_2 \dots dz_N \equiv f_N(\vec{z}_N) d\vec{z}_N \quad (65)$$

is the probability that particle 1 is between z_1 and $z_1 + dz_1$, particle 2 is between z_2 and $z_2 + dz_2$, etc. Without loss of generality, f_N can be considered invariant under the permutation of any two particles. As before, we compute the average $\langle J_x^2 \rangle_s$ in order to estimate the magnetic field gradient and also $\langle J_x^4 \rangle_s$ in order to estimate the uncertainty $\Delta\Theta$. For a general distribution function $f_N(\vec{z}_N)$, they are given by

$$\langle J_x^2 \rangle_s^{f_N}(\Theta) = \int d\vec{z}_N f_N(\vec{z}_N) \langle J_x^2 \rangle_s^{\vec{z}_N}(\Theta), \quad (66)$$

with $\langle J_x^2 \rangle_s^{\vec{z}_N}(\Theta)$ from Eq. (41), and

$$\langle J_x^4 \rangle_s^{f_N}(\Theta) = \int d\vec{z}_N f_N(\vec{z}_N) \langle J_x^4 \rangle_s^{\vec{z}_N}(\Theta), \quad (67)$$

with $\langle J_x^4 \rangle_s^{\bar{z}_N}(\Theta)$ from Eq. (59). Here and in the following, we substitute \bar{z}_N^c with \bar{z}_N in the expressions for fixed particle positions.

In order to compute particular examples, we need some properties of the reduced M -particle distribution functions f_M ($M \leq N$). These can be obtained from f_N as

$$f_M(\bar{z}_M) = \int dz_{M+1} \cdots dz_N f_N(\bar{z}_N), \quad (68)$$

where we used the shorthand notation $\bar{z}_M = (z_1, z_2, \dots, z_M)^T$ as above. Note that due to the invariance under permutations of f_N , it does not matter which of the $N - M$ particles are integrated over. Further, f_M is permutationally invariant as well.

A. Distributions with Dirac δ functions

For example, the distribution function of the chain considered in the previous section can be written as [62]

$$f_N^{\bar{z}_N^c}(\bar{z}_N) = \frac{1}{N!} \sum_{\neq(k_1, k_2, \dots, k_N)} \prod_{j=1}^N \delta(z_j - z_{k_j}^c). \quad (69)$$

Its reduced distribution functions are given by

$$f_M^{\bar{z}_M^c}(\bar{z}_M) = \frac{(N - M)!}{N!} \sum_{\neq(k_1, k_2, \dots, k_M)} \prod_{j=1}^M \delta(z_j - z_{k_j}^c). \quad (70)$$

The permutational invariance of f_M simplifies many calculations. For instance, the average of I_2 from Eq. (37) for a distribution $f_N(\bar{z}_N)$ becomes

$$\begin{aligned} \langle I_2 \rangle^{f_N} &= \int d\bar{z}_N I_2(\bar{z}_N) = \sum_{n \neq m} \int d\bar{z}_N f_N(\bar{z}_N) [c_n c_m + s_n s_m] \\ &= \sum_{n \neq m} \int dz_n dz_m f_2(z_n, z_m) [c_n c_m + s_n s_m] \\ &= N(N - 1) \int d\bar{z}_2 f_2(\bar{z}_2) [c_1 c_2 + s_1 s_2]. \end{aligned} \quad (71)$$

In analogy, we obtain the average of I_4 from Eq. (56) for $f_N(\bar{z}_N)$,

$$\begin{aligned} \langle I_4 \rangle^{f_N} &= \int d\bar{z}_N f_N(\bar{z}_N) I_4(\bar{z}_N) = \frac{N!}{(N - 4)!} \int d\bar{z}_4 f_4(\bar{z}_4) \\ &\quad \times [c_1 c_2 c_3 c_4 + s_1 s_2 s_3 s_4 + 2c_1 c_2 s_3 s_4]. \end{aligned} \quad (72)$$

With these, it is possible to recover all of our previous results for spin chains.

B. Independently and smoothly distributed particles

In the following, we will make the assumption that the system is a gas of particles that are uncorrelated in space, which means that the distribution function can be written as a product of single-particle distribution functions,

$$f_N^p(\bar{z}_N) = \prod_{n=1}^N f_1(z_n). \quad (73)$$

Further, we will assume that f_1 is a smooth function which does not contain Dirac δ functions, i.e., points with infinitely high density.

Let us compute the expectation values of J_x^2 and J_x^4 , as we did in the previous section, for a product distribution function of the form given in Eq. (73). Considering Eqs. (38) and (55), it becomes clear that we only need to compute $\langle I_2 \rangle^{f_N}$ and $\langle I_4 \rangle^{f_N}$. Since $f_2^p(\bar{z}_2) = f_1(z_1)f_1(z_2)$ in the uncorrelated case, we obtain from Eq. (71) that

$$\langle I_2 \rangle^{f_N^p} = N(N - 1)(\tilde{C}^2 + \tilde{S}^2), \quad (74)$$

where

$$\tilde{C} = \int dz_1 f_1(z_1) \cos\left(\frac{z_1}{L}\Theta\right) \quad (75)$$

and

$$\tilde{S} = \int dz_1 f_1(z_1) \sin\left(\frac{z_1}{L}\Theta\right). \quad (76)$$

Here the averaging is over the density distribution $f_1(z_1)$. With these, we have all of the ingredients to determine the dynamics of $\langle J_x^2 \rangle_s$ for the gas from Eq. (38).

Observation 5. For an ensemble of particles with a product distribution function f_N^p from Eq. (73), we obtain the following dynamics for the expectation value of the second moment of J_x :

$$\langle J_x^2 \rangle_s^{f_N^p}(\Theta) = \frac{N\hbar^2}{4} [1 - \tilde{C}^2 - \tilde{S}^2], \quad (77)$$

where \tilde{C} and \tilde{S} are defined in Eqs. (75) and (76).

In analogy, we obtain from Eq. (72) that

$$\langle I_4 \rangle^{f_N^p} = \frac{N!}{(N - 4)!} (\tilde{C}^2 + \tilde{S}^2)^2. \quad (78)$$

Inserting $\langle I_2 \rangle^{f_N^p}$ and $\langle I_4 \rangle^{f_N^p}$ into Eq. (55), we obtain the dynamics of $\langle J_x^4 \rangle_s$.

Observation 6. For an ensemble of particles with a product distribution function f_N^p from Eq. (73), we obtain the following dynamics for the expectation value for the fourth moment of J_x :

$$\begin{aligned} \langle J_x^4 \rangle_s^{f_N^p} &= \frac{N\hbar^4}{16} \{3N - 2 - (6N - 8)(\tilde{C}^2 + \tilde{S}^2) \\ &\quad + 3(N - 2)(\tilde{C}^2 + \tilde{S}^2)^2\}, \end{aligned} \quad (79)$$

where \tilde{C} and \tilde{S} are defined in Eqs. (75) and (76).

Note that due to the product structure of f_N^p , this expression is much simpler than the expression for the chain given in Eq. (59). These formulas make it possible already to calculate the precision of the phase estimation.

1. Gaussian density profile

One of the most common density profiles is the Gaussian profile. As an example, we will now calculate the dynamics for this case explicitly. The Gaussian density profile is given as

$$f_1^{\text{Gauss}}(z_1) = \frac{1}{\sqrt{2\pi\sigma^2}} e^{-\frac{(z_1 - z_0)^2}{2\sigma^2}}, \quad (80)$$

where z_0 is the coordinate of the point with the highest density and σ is the width of the profile. Substituting it into Eq. (77), we obtain

$$\tilde{C}^2 + \tilde{S}^2 = e^{-\frac{\sigma^2}{L^2}\Theta^2}, \quad (81)$$

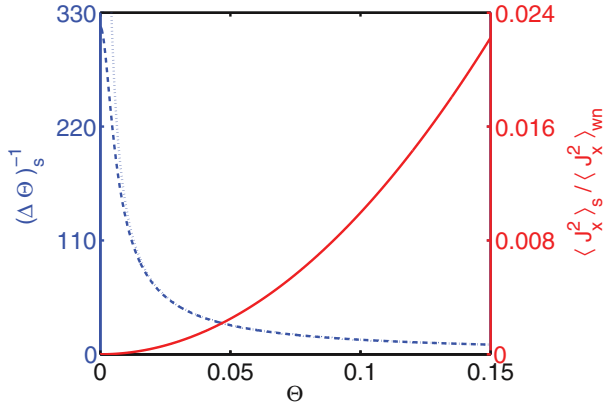


FIG. 3. (Color online) The dynamics of $\langle J_x^2 \rangle_s / \langle J_x^2 \rangle_{\text{wn}}$ (solid line) and $(\Delta\Theta)_s^{-1}$ (dashed line) as the function of Θ for $N = 10^5$ particles with a Gaussian density distribution [Eq. (80)] for $\sigma = L$. We also present $(\Delta\Theta)_s^{-1}$ calculated based on the Gaussianity assumption given by Eq. (111) discussed in Sec. VB (dotted line). The angular momentum variance for the white noise, $\langle J_x^2 \rangle_{\text{wn}}$, is defined in Eq. (45).

and hence

$$\langle J_x^2 \rangle_s^{f_N^p}(\Theta) = \frac{N\hbar^2}{4} (1 - e^{-\frac{\sigma^2}{L^2} \Theta^2}). \quad (82)$$

Note that the maximum of $\langle J_x^2 \rangle_s(\Theta)$ is exactly the value for white noise; cf. Eq. (45). Thus, in this case, there is no overshooting, and the noise does not become larger than that of the white noise, as was the case with the equidistant chain in Eq. (41).

In Fig. 3, we plot the dynamics of $\langle J_x^2 \rangle_s$ for $N = 10^5$ spin- $\frac{1}{2}$ particles. The density profile is a product distribution function of Gaussian profiles with $\sigma = L$.

2. Analytic formula for the maximum precision for any particle distribution, including correlated particle distributions

We will now give an analytic formula for the maximum precision at $\Theta = 0$ for the case of any particle distribution.

Observation 7. The maximal precision of estimating $\Delta\Theta$ is characterized by

$$(\Delta\Theta)_s^{-2}(\Theta = 0) = N \left[\frac{\sigma^2}{L^2} - \frac{\text{cov}(z_1, z_2)}{L^2} \right], \quad (83)$$

where

$$\begin{aligned} \sigma^2 &= \int dz f_1(z) (z - \langle z \rangle)^2, \quad \langle z \rangle = \int dz f_1(z) z, \\ \text{cov}(z_1, z_2) &= \int dz_1 dz_2 f_2(z_1, z_2) (z_1 - \langle z_1 \rangle) (z_2 - \langle z_2 \rangle). \end{aligned} \quad (84)$$

For the derivation, see the Supplemental Material [62]. For any product distribution function f_N^p , $(\Delta\Theta)_s^{-2}(\Theta = 0) = N \frac{\sigma^2}{L^2}$, since $\text{cov}(z_1, z_2) = 0$ in this case. Hence, the maximal sensitivity is a simple function of N and σ . Correlations can increase or decrease the sensitivity compared to the uncorrelated case. For instance, the correlations present in the equidistant chain increase $(\Delta\Theta)_s^{-2}(\Theta = 0)$ by a factor $\frac{N}{N-1}$; cf. Eq. (64).

V. FURTHER CONSIDERATIONS

A. The influence of noise

So far, we considered only perfect singlet states. In practice, the multipartite singlet state cannot be realized perfectly [64]. In this section, we will consider the case of starting from imperfect singlet states. First, we will discuss the case, when we measure $\langle J_x^2 \rangle$, as before. Then, we will show that a higher accuracy can be achieved in the noisy case, if other operators are measured.

1. Measuring the variance of an angular momentum component

A realistic method to model the imperfections is by introducing local decoherence channels for each qubit as

$$\epsilon_q^{(\text{wn})}(\varrho) = (1 - q)\varrho + q \frac{\mathbb{1}}{2}, \quad (85)$$

where $0 \leq q \leq 1$. Each spin is mixed with a certain amount of white noise locally. The above single-qubit decoherence is given by the Kraus operators as $\epsilon_q^{(\text{wn})}(\varrho) = (1 - q)\varrho + q \sum_i K_i \varrho K_i^\dagger$, where $\mathbf{K} = \{\mathbb{1}, \sigma_x, \sigma_y, \sigma_z\}/2$.

We assume that all these decoherence channels act in parallel for all spins. Thus, we obtain the multispin decoherence,

$$\mathcal{E}_q^{(\text{wn})}(\varrho) = \epsilon_q^{(\text{wn},1)}(\varrho) \circ \epsilon_q^{(\text{wn},2)}(\varrho) \circ \dots \circ \epsilon_q^{(\text{wn},N)}(\varrho). \quad (86)$$

In Eq. (86), \circ indicates function composition $(f \circ g)(x) = f(g(x))$ and the number in the superscript indicates to which qubit the function is applied. We consider an atomic ensemble with a continuous distribution. Next we outline briefly the derivation of the noisy dynamics for this case.

The moments $\langle J_x^2 \rangle$ and $\langle J_x^4 \rangle$ given in Eqs. (33) and (52), respectively, are affected through the two-body and four-body correlations via the formulas

$$\sum_{n_1 \neq n_2} \langle X_\Theta^{(n_1)} X_\Theta^{(n_2)} \rangle_{\varrho_{s,\text{wn}}} = (1 - q)^2 \sum_{n_1 \neq n_2} \langle X_\Theta^{(n_1)} X_\Theta^{(n_2)} \rangle_{\varrho_s} \quad (87)$$

and

$$\begin{aligned} &\sum_{\neq(n_1, n_2, n_3, n_4)} \langle X_\Theta^{(n_1)} X_\Theta^{(n_2)} X_\Theta^{(n_3)} X_\Theta^{(n_4)} \rangle_{\varrho_{s,\text{wn}}} \\ &= (1 - q)^4 \sum_{\neq(n_1, n_2, n_3, n_4)} \langle X_\Theta^{(n_1)} X_\Theta^{(n_2)} X_\Theta^{(n_3)} X_\Theta^{(n_4)} \rangle_{\varrho_s}. \end{aligned} \quad (88)$$

Hence, for the atomic cloud, we obtain (cf. Observations 5 and 6)

$$\langle J_x^2 \rangle_{s,\text{wn}}^{f_N^p}(q) = \frac{N\hbar^2}{4} [1 - (1 - q)^2 (\tilde{C}^2 + \tilde{S}^2)] \quad (89)$$

and

$$\begin{aligned} \langle J_x^4 \rangle_{s,\text{wn}}^{f_N^p}(q) &= \frac{N\hbar^4}{16} \{3N - 2 - (1 - q)^2 (6N - 8) (\tilde{C}^2 + \tilde{S}^2) \\ &\quad + (1 - q)^4 3(N - 2) (\tilde{C}^2 + \tilde{S}^2)^2\}. \end{aligned} \quad (90)$$

Note that for $q = 1$, Eqs. (89) and (90) reduce to the values corresponding to a global white noise. Equation (89) can be rewritten as

$$\langle J_x^2 \rangle_{s,\text{wn}}(q) = (1 - q)^2 \langle J_x^2 \rangle_s + [1 - (1 - q)^2] \langle J_x^2 \rangle_{\text{wn}}. \quad (91)$$

Let us consider a Gaussian density profile described in Sec. IV B1 for which we have $\tilde{C}^2 + \tilde{S}^2$ given in Eq. (81).

Substituting Eq. (81) into Eqs. (89) and (90), we can compute the influence of the noise for the second and fourth moments of the angular momentum components. The precision of the reconstruction of Θ based on measuring J_x^2 can be obtained as

$$(\Delta\Theta)_{s,wn}^2 = \frac{\langle J_x^4 \rangle_{s,wn}(\Theta) - \langle J_x^2 \rangle_{s,wn}(\Theta)^2}{(1-q)^4 |\partial_\Theta \langle J_x^2 \rangle_s|^2}. \quad (92)$$

Let us see now the behavior of the precision given by Eq. (92) under noise in the limiting cases, for $q > 0$.

(i) At $\Theta = 0$, the denominator of the right-hand side of Eq. (92) is zero. This can be seen from Eq. (44), from which it follows that $\partial_\Theta \langle J_x^2 \rangle_s$ is a sum of sine expressions, which vanish at $\Theta = 0$. In contrast, the numerator is a positive number. Hence, even for very small amount of noise, we have

$$(\Delta\Theta)_{s,wn}^{-2}(\Theta = 0) = 0. \quad (93)$$

Note that this is due to the fact that we chose a noise state which is invariant under the Θ -dependent transformation U_G from Eq. (27). The precision remains close to zero until the noise of the singlet becomes comparable to the added noise.

(ii) The other limit is the case of the large Θ . Let us define Θ_{wn} such that for $\Theta > \Theta_{wn}$ the singlet evolved into a state that, based on the second and fourth moments of the angular momentum coordinates, is like the completely mixed state. That is, for $\Theta > \Theta_{wn}$, we have

$$\langle J_x^2 \rangle_s(\Theta) \approx \langle J_x^2 \rangle_{wn}, \quad \langle J_x^4 \rangle_s(\Theta) \approx \langle J_x^4 \rangle_{wn}. \quad (94)$$

The reason for this is that for large enough Θ , the quantity $\tilde{C}^2 + \tilde{S}^2$ as given in Eq. (81) is close to zero, and in Eqs. (89) and (90) only the constant terms corresponding to the moments of the white noise remain. Hence, based on Eq. (92) for $\Theta > \Theta_{wn}$, we have

$$(\Delta\Theta)_{s,wn}^{-2}(\Theta) \approx (1-q)^4 (\Delta\Theta)_s^{-2}(\Theta). \quad (95)$$

In Fig. 4, we calculated the precision $(\Delta\Theta)_{s,wn}(\Theta)$ as a function of the noise for $q = 0.01, 0.05$, and 0.1 for a Gaussian ensemble. For these values, for large Θ ,

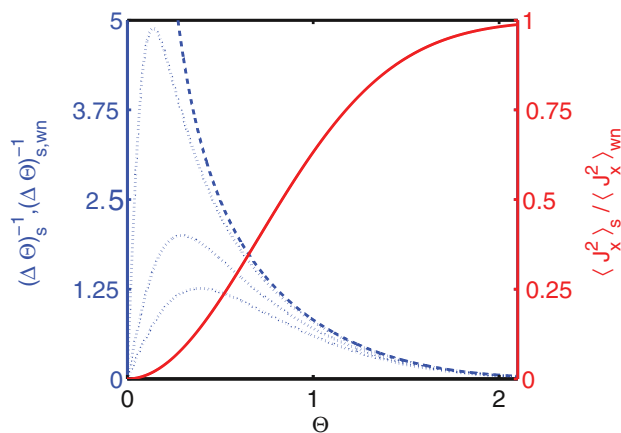


FIG. 4. (Color online) The dynamics of $\langle J_x^2 \rangle_s / \langle J_x^2 \rangle_{wn}$ (solid line) and the precision $(\Delta\Theta)_s^{-1}$ for the noiseless case (dashed line) and $(\Delta\Theta)_{s,wn}^{-1}$ for a noise with $q = 0.01, 0.05$ and 0.1 (from top to bottom, dotted line) as the function of Θ for $N = 10^5$ particles. $\langle J_x^2 \rangle_{wn}$ is defined in Eq. (45). The density profile is Gaussian and $\sigma = L$.

we have $(\Delta\Theta)_s^{-2}(\Theta) / (\Delta\Theta)_{s,wn}^{-2}(\Theta) = 1.04, 1.23$, and 1.52 , respectively.

2. Measuring operators different from the angular momentum components

We will show a simple example that even in the noisy case, a higher accuracy of the gradient estimation can be achieved if quantities other than $\langle J_x^2 \rangle$ are measured. Let us consider a noisy singlet of the type

$$\varrho_{ns} = p_n \frac{\mathbb{1}}{2^N} + (1 - p_n) \varrho_s. \quad (96)$$

Let us now look at the projector to the $J_x = 0$ subspace. For the completely mixed state, the expectation value of the projector is

$$\langle P_{J_x=0} \rangle_n = 2^{-N} \binom{N}{\frac{N}{2}} \approx \sqrt{\frac{2}{\pi}} \frac{1}{\sqrt{N}}, \quad (97)$$

while for the singlet, we have $\langle P_{J_x=0} \rangle_s(\Theta = 0) = 1$. Hence, for the noisy state, we obtain

$$\langle P_{J_x=0} \rangle_{ns} \approx p_n \sqrt{\frac{2}{\pi}} \frac{1}{\sqrt{N}} + (1 - p_n) \langle P_{J_x=0} \rangle_s. \quad (98)$$

During the dynamics, based on Eq. (98), the expectation value of the projector $\langle P_{J_x=0} \rangle_s$ decreases from 1 to a value close to zero, while the noise in the expectation value of the projector $\langle P_{J_x=0} \rangle_n$ is proportional to $N^{-\frac{1}{2}}$, i.e., it is $O(N^{-\frac{1}{2}})$. In contrast, if the second moment $\langle J_x^2 \rangle$ is measured, then

$$\langle J_x^2 \rangle_{ns} = p_n \frac{N\hbar^2}{4} + (1 - p_n) \langle J_x^2 \rangle_s. \quad (99)$$

Based on Eq. (99), $\langle J_x^2 \rangle_s$ changes from 0 to a value close to $O(N)$, while the noise in the expectation value of the second moment $\langle J_x^2 \rangle_n$ is of the same order, $O(N)$. It can be seen that the effect of the noise is much smaller in the expectation value of the projector (98) than in the second moment (99). An analogous calculation can be carried out for local noise channels for operators of the type $P_{J_x=\text{const}}$.

B. Spin- j particles

So far we have discussed the case of singlet states of $j = \frac{1}{2}$ particles. In this section, we will study the singlet of spin- j particles. We will find that the dynamics of $\langle J_x^2 \rangle$ for N spin- j particles is the same as the dynamics of $\langle J_x^2 \rangle$ for N spin- $\frac{1}{2}$ particles, when in both cases we normalize the variance with that of the white noise. Moreover, we find that by using a certain Gaussian assumption in order to estimate $\langle J_x^4 \rangle_s$, we obtain the same dynamics even for the precision.

When considering the spin- j case, one could think about using the ideas of Observation 1 to obtain the multiparticle singlet of spin- j particles as an equal mixture of all the permutations of tensor products of two-particle singlets. However, the state obtained this way does not equal Eq. (7). This is due to the fact that for $j > \frac{1}{2}$, there are several permutationally invariant $SU(2)$ singlets [65]. Hence, for $j > \frac{1}{2}$, another method is needed.

For the dynamics of the variance of the collective angular momentum components, we need again the variance for the

completely mixed state (white noise), which is obtained for N spin- j particles as

$$\langle J_x^2 \rangle_{\text{wn},j} = \frac{Nj(j+1)}{3} \hbar^2. \quad (100)$$

Note that $\langle J_x^2 \rangle_{\text{wn},\frac{1}{2}} = \langle J_x^2 \rangle_{\text{wn}}$, where $\langle J_x^2 \rangle_{\text{wn}}$ is defined in Eq. (45). As we will see, the dynamics of the variance of the singlet will be similar to the dynamics for the $j = \frac{1}{2}$ case, apart from a factor of

$$\kappa_j = \frac{\langle J_x^2 \rangle_{\text{wn},j}}{\langle J_x^2 \rangle_{\text{wn}}} = \frac{4}{3} j(j+1), \quad (101)$$

and hence, for large Θ , we will have $\langle J_x^2 \rangle_{s,j}(\Theta) \approx \langle J_x^2 \rangle_{\text{wn},j}$.

Let us denote by j_l the angular momentum components of a single spin- j particle. Since for each spin the dynamics is invariant under a coordinate transformation, from $(j_x^{(n)})^2 + (j_y^{(n)})^2 + (j_z^{(n)})^2 = j(j+1)\hbar^2$, we obtain

$$\left\langle \sum_n (j_l^{(n)})^2 \right\rangle(\Theta) = \langle J_x^2 \rangle_{\text{wn},j}, \quad (102)$$

for $l = x, y, z$ and for all Θ . Moreover, from the requirement that $\langle J_l^2 \rangle_{s,j} = 0$, we obtain

$$\langle J_x^2 \rangle = \left\langle \sum_n (j_z^{(n)})^2 \right\rangle_{s,j} + N(N-1) \langle j_l^{(1)} j_l^{(2)} \rangle_{s,j} = 0. \quad (103)$$

Note that $\langle j_l^{(1)} j_l^{(2)} \rangle_{s,j} = \langle j_l^{(n)} j_l^{(n')} \rangle_{s,j}$ for $n \neq n'$ due to the permutational invariance of the state. Hence, we arrive at

$$\langle j_l^{(n)} j_l^{(n')} \rangle_{s,j} = -\frac{\langle J_x^2 \rangle_{\text{wn},j}}{N(N-1)}, \quad (104)$$

and we can rewrite Eq. (35) for particles with $j > \frac{1}{2}$ as

$$\langle j_k \otimes j_l \rangle_{\varrho_{12}^{\text{red},j}} = -\frac{\langle J_x^2 \rangle_{\text{wn},j}}{N(N-1)} \delta_{kl}, \quad (105)$$

where $\varrho_{12}^{\text{red},j}$ is now the reduced state of the spin- j singlet [63].

The time-evolved single-particle operators $j_x(\Theta) \equiv X(\Theta)$ have the same form as in the $j = \frac{1}{2}$ case, given in Eq. (30). Therefore, we can perform the calculation for any j in analogy to the derivation for the spin- $\frac{1}{2}$ case of Sec. III A. Starting from

$$\langle J_x^2(\Theta) \rangle_{s,j} = \langle J_x^2 \rangle_{\text{wn},j} + \sum_{n_1 \neq n_2} \langle X_{\Theta}^{(n_1)} X_{\Theta}^{(n_2)} \rangle_{s,j}, \quad (106)$$

we arrive at

$$[\langle J_x^2(\Theta) \rangle]_{s,j} = \kappa_j [\langle J_x^2(\Theta) \rangle]_s. \quad (107)$$

Therefore, Observation 2 generalizes to spin- j particles as follows.

Observation 8. The dynamics of the variance of J_x for a chain of spin- j particles with the z coordinates \vec{z}_N^c is

$$\langle J_x^2 \rangle_{s,j}^{\vec{z}_N^c}(\Theta) = \kappa_j \frac{\hbar^2 N}{4} \left\{ 1 + \frac{1}{N(N-1)} [N - C^2 - S^2] \right\}, \quad (108)$$

where C and S are defined in Eq. (40).

For an ensemble of particles with a density profile $\lambda(z)$, we can in analogy generalize Observation 5 to any j as follows.

Observation 9. For an ensemble of spin- j particles with a product distribution function f_N^p from Eq. (73), we obtain the following dynamics for the expectation value of the second moment of J_x :

$$\langle J_x^2 \rangle_s^{f_N^p}(\Theta) = \kappa_j \frac{N\hbar^2}{4} [1 - \tilde{C}^2 - \tilde{S}^2], \quad (109)$$

where \tilde{C} and \tilde{S} are defined in Eqs. (75) and (76). Here the averaging is over the density distribution $f_1(z_1)$.

For the Gaussian density profile (80), we arrive at

$$\langle J_x^2 \rangle(\Theta) = \kappa_j \frac{N}{4} \hbar^2 (1 - e^{-\frac{\sigma^2}{L^2} \Theta^2}). \quad (110)$$

The calculation of $\langle J_x^4 \rangle(\Theta)$ for the singlet of spin- j particles seems to be much more complicated than for spin- $\frac{1}{2}$ particles. It is possible to avoid calculating the fourth-order moment by using the assumption that when J_x is measured, the probability of the measurement outcomes follows a Gaussian curve, with the zero outcome being the most probable. For such Gaussian probability distributions, the higher-order moments can be obtained from second-order ones [66]. In particular, for our case,

$$\langle J_x^4 \rangle \approx 3 \langle J_x^2 \rangle^2. \quad (111)$$

Equation (111) leads to $(\Delta J_x^2)^2 \approx 2 \langle J_x^2 \rangle^2$, keeping in mind that $\langle J_x \rangle = 0$. Such a Gaussianity assumption is expected to work for later times, as at $\Theta = 0$ the variance of J_x is zero, and in the beginning only a few of the eigenstates of J_x are populated. Later, however, many eigenstates of J_x are populated and a continuous approximation of the discrete spectrum is appropriate. Note that the Gaussianity of the probability distribution is a notion completely independent from the Gaussianity of the density profile of the cold gas.

One can substitute the Gaussian assumption (111) into the formula for $(\Delta \Theta)_s^2$ given in Eq. (48), which can be used for any j . This clearly simplifies the calculations. For the accuracy of gradient metrology for N spin- j particles, we obtain the same result as for N spin- $\frac{1}{2}$ particles,

$$(\Delta \Theta)_{s,j}(\Theta) = (\Delta \Theta)_{s,\frac{1}{2}}(\Theta). \quad (112)$$

In Fig. 3, besides the exact result, we also plot the dynamics based on the approximation using the Gaussian assumption on the correlations given by Eq. (111) for the $j = \frac{1}{2}$ case as an illustration. The bound obtained this way diverges at $t = 0$; however, it is very close to the true value for $\Theta > 0.025$. We also carried out a calculation for $j > \frac{1}{2}$. In Fig. 5, one can see the comparison for the case of a chain of six spin-1 particles. The precision based on the Gaussian assumption diverges at $t = 0$; however, it later fits the exact dynamics very well.

VI. Discussion and Conclusion

We presented calculations for a many-particle singlet in a magnetic field gradient for an ensemble of distinguishable, well-localized spin- $\frac{1}{2}$ particles. We have shown that multiparticle singlets created in cold atomic ensembles can be used for differential magnetometry. The magnetic field gradient can be estimated by measuring the variance of one of the components of the collective angular momentum. We

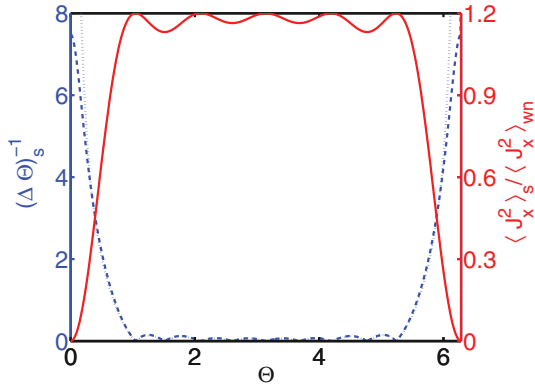


FIG. 5. (Color online) The dynamics of $\langle J_x^2 \rangle_s / \langle J_x^2 \rangle_{\text{wn}}$ (solid line) and $(\Delta\Theta)_s^{-1}$ (dashed line) as the function of Θ for $N = 6$ spin-1 particles in an equidistant chain. We also present $(\Delta\Theta)_s^{-1}$ calculated based on the Gaussianity assumption given by Eq. (111) discussed in Sec. VB (dotted line).

calculated the dependence of this variance on the field gradient and the measurement time. We also calculated the precision of the estimation of the field gradient. We have also considered admixtures of white noise and discussed the extension of the results for general spin- j particles. Our work opens up the possibilities for experiments with unpolarized ensembles.

In the future, it would be interesting to find bounds for the precision of the field gradient measurements using the theory of the quantum Fisher information [67]. It is an

interesting question as to whether the accuracy of parameter estimation in our calculations saturates the accuracy bound determined by the quantum Fisher information. It would also be important to consider the case of particles that are not well localized, in which case the spatial degree of freedom cannot be easily separated from the internal degrees of freedom for the quantum dynamics we considered [67]. For room-temperature experiments with atomic ensembles, the atoms must be well localized; however, singlets can also be realized with Bose-Einstein condensates, for which all particles are delocalized. For such systems, the noise is very different from the case of distinguishable particles. Finally, the effect of a field gradient could be used to examine symmetric Dicke states with $\langle J_z \rangle = 0$ rather than singlets [41,42]. Our calculations could be generalized to that case.

ACKNOWLEDGMENTS

We thank J. Calsamiglia, G. Colangelo, O. Guhne, M. Modugno, L. Santos, R. J. Sewell, and Z. Zimboras for discussions. We thank the European Union (ERC Starting Grants GEDENTQOPT and AQUMET, CHIST-ERA QUASAR), the Spanish MINECO (Projects No. FIS2009-12773-C02-02, No. FIS2012-36673-C03-03 and No. FIS2011-23520), the Basque Government (Projects No. IT4720-10 and No. IT559-10), and the support of the National Research Fund of Hungary OTKA (Contract No. K83858). I.U.L. acknowledges the support of a Ph.D. grant of the Basque Government.

- [1] J. Hald, J. L. Sorensen, C. Schori, and E. S. Polzik, *Phys. Rev. Lett.* **83**, 1319 (1999).
- [2] B. Julsgaard, A. Kozhekin, and E. S. Polzik, *Nature (London)* **413**, 400 (2001).
- [3] V. Meyer, M. A. Rowe, D. Kielpinski, C. A. Sackett, W. M. Itano, C. Monroe, and D. J. Wineland, *Phys. Rev. Lett.* **86**, 5870 (2001).
- [4] K. Hammerer, A. S. Sorensen, and E. S. Polzik, *Rev. Mod. Phys.* **82**, 1041 (2010).
- [5] L. M. Duan, J. I. Cirac, P. Zoller, and E. S. Polzik, *Phys. Rev. Lett.* **85**, 5643 (2000).
- [6] A. Kuzmich, N. P. Bigelow, and L. Mandel, *Europhys. Lett.* **42**, 481 (1998).
- [7] J. F. Sherson, H. Krauter, R. K. Olsson, B. Julsgaard, K. Hammerer, I. Cirac, and E. S. Polzik, *Nature (London)* **443**, 557 (2006).
- [8] W. Wasilewski, K. Jensen, H. Krauter, J. J. Renema, M. V. Balabas, and E. S. Polzik, *Phys. Rev. Lett.* **104**, 133601 (2010).
- [9] K. Eckert, P. Hyllus, D. Bruss, U. V. Poulsen, M. Lewenstein, C. Jentsch, T. Muller, E. M. Rasel, and W. Ertmer, *Phys. Rev. A* **73**, 013814 (2006).
- [10] F. Wolfgramm, A. Cere, F. A. Beduini, A. Predojevic, M. Koschorreck, and M. W. Mitchell, *Phys. Rev. Lett.* **105**, 053601 (2010).
- [11] R. J. Sewell, M. Koschorreck, M. Napolitano, B. Dubost, N. Behbood, and M. W. Mitchell, *Phys. Rev. Lett.* **109**, 253605 (2012).
- [12] V. Shah, G. Vasilakis, and M. V. Romalis, *Phys. Rev. Lett.* **104**, 013601 (2010).
- [13] T. Horrom, R. Singh, J. P. Dowling, and E. E. Mikhailov, *Phys. Rev. A* **86**, 023803 (2012).
- [14] G. Giedke and J. I. Cirac, *Phys. Rev. A* **66**, 032316 (2002).
- [15] L. B. Madsen and K. Molmer, *Phys. Rev. A* **70**, 052324 (2004).
- [16] K. Hammerer, K. Molmer, E. S. Polzik, and J. I. Cirac, *Phys. Rev. A* **70**, 044304 (2004).
- [17] S. R. de Echaniz, M. W. Mitchell, M. Kubasik, M. Koschorreck, H. Crepaz, J. Eschner, and E. S. Polzik, *J. Opt. B* **7**, S548 (2005).
- [18] M. Koschorreck and M. W. Mitchell, *J. Phys. B* **42**, 195502 (2009).
- [19] M. Kitagawa and M. Ueda, *Phys. Rev. A* **47**, 5138 (1993).
- [20] D. J. Wineland, J. J. Bollinger, W. M. Itano, and D. J. Heinzen, *Phys. Rev. A* **50**, 67 (1994).
- [21] A. S. Sorensen, L. M. Duan, J. I. Cirac, and P. Zoller, *Nature (London)* **409**, 63 (2001).
- [22] J. Ma, X. Wang, C. P. Sun, and F. Nori, *Phys. Rep.* **509**, 89 (2011).
- [23] S. T. Keenan and E. J. Romans, *NDT&E Int.* **47**, 1 (2012).
- [24] H. Cable and G. A. Durkin, *Phys. Rev. Lett.* **105**, 013603 (2010).
- [25] G. Toth and M. W. Mitchell, *New J. Phys.* **12**, 053007 (2010).
- [26] N. Behbood, M. Napolitano, G. Colangelo, B. Dubost, S. Palacios lvarez, R. Sewell, G. Toth, and M. Mitchell, in *Research in Optical Sciences*, OSA Technical Digest No. QM1B.2 (Optical Society of America, Washington, DC, 2012).
- [27] W. Yao, *Phys. Rev. B* **83**, 201308(R) (2011).
- [28] R. N. Stevenson, J. J. Hope, and A. R. R. Carvalho, *Phys. Rev. A* **84**, 022332 (2011).
- [29] J. Meineke, J.-P. Brantut, D. Stadler, T. Muller, H. Moritz, and T. Esslinger, *Nat. Phys.* **8**, 455 (2012).

- [30] K. Eckert, O. Romero-Isart, M. Rodríguez, M. Lewenstein, E. S. Polzik, and A. Sanpera, *Nat. Phys.* **4**, 50 (2008).
- [31] T. Keilmann and J. J. García-Ripoll, *Phys. Rev. Lett.* **100**, 110406 (2008).
- [32] K. Ueda, H. Kontani, M. Sigrist, and P. A. Lee, *Phys. Rev. Lett.* **76**, 1932 (1996).
- [33] S. Miyahara and K. Ueda, *Phys. Rev. Lett.* **82**, 3701 (1999).
- [34] M. Lubasch, V. Murg, U. Schneider, J. I. Cirac, and M.-C. Bañuls, *Phys. Rev. Lett.* **107**, 165301 (2011).
- [35] M.-K. Zhou, Z.-K. Hu, X.-C. Duan, B.-L. Sun, J.-B. Zhao, and J. Luo, *Phys. Rev. A* **82**, 061602(R) (2010).
- [36] S. Wildermuth, S. Hofferberth, I. Lesanovsky, S. Groth, P. Krüger, and J. Schmiedmayer, *Appl. Phys. Lett.* **88**, 264103 (2006).
- [37] M. Vengalattore, J. M. Higbie, S. R. Leslie, J. Guzman, L. E. Sadler, and D. M. Stamper-Kurn, *Phys. Rev. Lett.* **98**, 200801 (2007).
- [38] M. Koschorreck, M. Napolitano, B. Dubost, and M. W. Mitchell, *Appl. Phys. Lett.* **98**, 074101 (2011).
- [39] N. Behbood, F. Martin Ciurana, G. Colangelo, M. Napolitano, M. W. Mitchell, and R. J. Sewell, *Appl. Phys. Lett.* **102**, 173504 (2013).
- [40] B. Dubost, M. Koschorreck, M. Napolitano, N. Behbood, R. J. Sewell, and M. W. Mitchell, *Phys. Rev. Lett.* **108**, 183602 (2012).
- [41] B. Lücke, M. Scherer, J. Kruse, L. Pezzé, F. Deuretzbacher, P. Hyllus, O. Topic, J. Peise, W. Ertmer, J. Arlt, L. Santos, A. Smerzi, and C. Klempt, *Science* **334**, 773 (2011).
- [42] C. D. Hamley, C. S. Gerving, T. M. Hoang, E. M. Bookjans, and M. S. Chapman, *Nat. Phys.* **8**, 305 (2012).
- [43] A. B. Klimov, H. Tavakoli Dinani, Z. E. D. Medendorp, and H. de Guise, *New J. Phys.* **13**, 113033 (2011).
- [44] J. D. Sau, S. R. Leslie, M. L. Cohen, and D. M. Stamper-Kurn, *New J. Phys.* **12**, 085011 (2010).
- [45] G. I. Mias, N. R. Cooper, and S. M. Girvin, *Phys. Rev. A* **77**, 023616 (2008).
- [46] Z. Kurucz and K. Mølmer, *Phys. Rev. A* **81**, 032314 (2010).
- [47] D. M. Stamper-Kurn and M. Ueda, arXiv:1205.1888.
- [48] A. S. Sørensen and K. Mølmer, *Phys. Rev. Lett.* **86**, 4431 (2001).
- [49] L.-M. Duan, J. I. Cirac, and P. Zoller, *Phys. Rev. A* **65**, 033619 (2002).
- [50] Ö. E. Müstecaplıoğlu, M. Zhang, and L. You, *Phys. Rev. A* **66**, 033611 (2002).
- [51] G. Tóth, *Phys. Rev. A* **69**, 052327 (2004).
- [52] M. Wieśniak, V. Vedral, and Č. Brukner, *New J. Phys.* **7**, 258 (2005).
- [53] G. Vitagliano, P. Hyllus, I. L. Egusquiza, and G. Tóth, *Phys. Rev. Lett.* **107**, 240502 (2011).
- [54] Q. Y. He, S.-G. Peng, P. D. Drummond, and M. D. Reid, *Phys. Rev. A* **84**, 022107 (2011).
- [55] J. I. Cirac, A. K. Eckert, and C. Macchiavello, *Phys. Rev. Lett.* **82**, 4344 (1999).
- [56] G. Tóth, W. Wieczorek, D. Gross, R. Krischek, C. Schwemmer, and H. Weinfurter, *Phys. Rev. Lett.* **105**, 250403 (2010).
- [57] Alternatively, one can argue based on the group theory of angular momentum. Let us write the permutationally invariant density matrix in the usual block-diagonal form. Here, SU(2) operations act within the blocks, while permutations act between the blocks. For the permutationally invariant case, all blocks corresponding to the same j and j_z are the same. The block size corresponding to $j = 0$ is 1×1 . Thus, all permutationally invariant states can be written as $\varrho = (1 - p_s)\varrho_{>0} + p_s\varrho_s$, where $0 \leq p_s \leq 1$, ϱ_s is defined in Eq. (8), and $\varrho_{>0}$ is a permutationally invariant state not having a contribution in the $J^2 = 0$ subspace. For a very clear presentation of the group theoretical basis for this statement in another context, see R. B. A. Adamson, P. S. Turner, M. W. Mitchell, and A. M. Steinberg, *Phys. Rev. A* **78**, 033832 (2008). This comment is based on J. Calsamiglia (private communication).
- [58] Note that it has been known that a multiparticle singlet is within the space of the tensor products of two-particle singlets for $j = \frac{1}{2}$ [55]. Here we have shown that the state given by Eq. (7) is an *equal* mixture of such states. One can see even by simple numerics for small systems that an analogous condition does not hold for $j > \frac{1}{2}$.
- [59] Note that while there are $N!$ different permutation operators, there are only $(N + 1)!! = (N + 1)(N - 1)(N - 3) \dots$ different permutations of the tensor product of two-particle singlets. This can be proved as follows. We call $f(N)$ the number of different pairings for N particles. First, pair the first and the second particle. We will still have $f(N - 2)$ possibilities of pairing all the remaining particles among each other. So, we have $f(N) = f(N - 2) + \text{other contributions}$. Second, we pair the first particle with the third one. Again we will have $f(N - 2)$ possibilities of pairing the remaining spins. So, $f(N) = 2f(N - 2) + \text{other contributions}$. Then we pair the first particle with the fourth one, and again $f(N - 2)$ particles. We can repeat this procedure until we have paired the first particle with all of the others in the chain. As there are $N - 1$ particles that are not the first particle, in the end we will have $f(N) = (N - 1)f(N - 2)$. We also know that $f(2) = 1$, since for two particles there is only one possible pairing. Solving this recurrence relation, we get $f(N) = (N - 1)!!$. Note that we are careful and do not double count the permutations.
- [60] M. Greiner, O. Mandel, T. Esslinger, T. W. Hänsch, and I. Bloch, *Nature (London)* **415**, 39 (2002).
- [61] O. Morsch and M. Oberthaler, *Rev. Mod. Phys.* **78**, 179 (2006).
- [62] See Supplemental Material at <http://link.aps.org/supplemental/10.1103/PhysRevA.88.013626> for additional derivations.
- [63] The fact that $\langle j_k \otimes j_l \rangle_{\varrho_{12}^{\text{red},j}} = 0$ for $k \neq l$ follows from the SU(2) invariance of $\varrho_{12}^{\text{red},j}$ because a rotation around k by π leads to $j_k \rightarrow j_k$, but $j_l \rightarrow -j_l$, whence $\langle j_k \otimes j_l \rangle_{\varrho_{12}^{\text{red},j}} = -\langle j_k \otimes j_l \rangle_{\varrho_{12}^{\text{red},j}}$. In analogy, it follows that $\langle j_x^{(1)} j_y^{(2)} j_y^{(3)} j_y^{(4)} \rangle_{\rho_{1234}^{\text{red}}} = \langle j_x^{(1)} j_x^{(2)} j_x^{(3)} j_x^{(4)} \rangle_{\rho_{1234}^{\text{red}}} = 0$ as used in Sec. III B.
- [64] Noise can have a strong impact on quantum metrological setups. See R. Demkowicz-Dobrzański, J. Kołodyński, and M. Guta, *Nat. Comm.* **3**, 1063 (2012).
- [65] Note that there is still a unique permutationally invariant SU(d) singlet for a system of d -dimensional particles.
- [66] For a Gaussian probability distribution, the first- and second-order moments determine all higher-order moments. Thus, if the outcome statistics of the J_x measurement is Gaussian, the fourth moment $\langle J_x^4 \rangle$ can be obtained from the second moment $\langle J_x^2 \rangle$ as $\langle J_x^4 \rangle = 3\langle J_x^2 \rangle^2$.
- [67] I. Apellaniz and P. Hyllus (unpublished).